EFFECT OF SURFACTANT ADDITION ON PROPERTIES AND IN-VITRO BEHAVIOUR OF TETRACALCIUM PHOSPHATE-NANOMONETITE CEMENTS

Ľ. Medvecký, M. Giretová, R. Štulajterová, Z. Danková

Abstract

Tetracalcium phosphate - nanomonetite cements have been prepared by reaction milling of tetracalcium phosphate with orthophosphoric acid ethanol solution, which was modified with different water content. The presence of nanomonetite phase significantly reduced the pH value of cement pastes during hardening. The fast transformation of reactants in cement powder mixtures was observed during hardening and no reactants were found in cements after 24 hours of hardening. The SDS addition influenced the microstructure and hydroxyapatite particle morphology in cement. The highest compressive strength (35 MPa) was measured in cement prepared without an SDS addition. The SDS adsorption on particles of powder mixtures caused a lowering of mechanical strength. Excellent initial cell attachment without any visible cytotoxicity and good osteoblast proliferation were observed on surfaces of cements synthesized from powders with water addition. Osteoblasts were well spread on surfaces with clearly visible filopodia. No initial cytotoxicities were observed. The cement with the SDS addition had lower osteoblast proliferation and ALP activity with prolongation of culturing.

Keywords: tetracalcium phosphate, monetite, microstructure, sodium dodecyl sulfate, hardening; in-vitro tests

INTRODUCTION

Calcium phosphate cements (CPC) based on tetracalcium phosphate (TTCP) are composed of basic (TTCP) and acidic (e.g. brushite or monetite (DCPA)) components, which mutually interact to the final product - calcium-deficient hydroxyapatite (CDHA) after the addition of hardening liquid [1]. It has been shown that the CPC compressive strength and the solution pH increase with soaking time [2]. TTCP cements showed better antimicrobial activity than the calcium hydroxide [3]. CPC can contain residual TTCP after hardening [4] because of the formation of a dense hydroxyapatite layer on the surface of TTCP particles [5]. It was confirmed that the dissolution of DCPA in the first stage of the hardening process and consequently TTCP dissolution are significant factors which affect the transformation rate of cement components [6]. The cement paste with DCPA synthesized by a short time mixing of orthophosphoric acid aqueous solution with TTCP powder showed a high value of compressive strength and a faster formation of apatite phase [7]. The rise in in-vitro alkaline phosphatase (ALP) activity and a good proliferation of cells were found in macroporous scaffolds prepared from CPC [8]. TTCP showed no significant influence on cell proliferation but the increase in ALP activity and osteogenesis promotion

Ľubomír Medvecký, Mária Giretová, Radoslava Štulajterová, Institute of Materials Research, Slovak Academy of Sciences, Košice, Slovak Republic
Zuzana Danková, Institute of Geotechnics, Slovak Academy of Sciences, Košice, Slovak Republic

were verified [9]. The addition of sodium dodecyl sulphate (SDS) to the sodium hydrogen phosphate hardening liquid caused the formation of macroporosity in the cements and a decrease of both the hydroxyapatite crystallinity and particle sizes in cements [10]. Similarly, Sarda et al. [11] used SDS as an air trapping agent, which allowed control of macroporosity in CPC via SDS concentration in the hardening liquid.

In this paper, we studied the influence of preadsorbed sodium dodecylsulphate on the particle morphology and phase composition, hardening process, microstructure, mechanical properties of tetracalcium-nanomonetite cements. Besides the in-vitro testing using MC3T3 pre-osteoblasts there were carried out on hardened cements for evaluation of their cytotoxicity and ALP activity as a marker of new bone formation.

MATERIALS AND METHODS

Tetracalcium phosphate ($Ca_4(PO_4)_2O$, TTCP) was prepared by annealing an equimolar mixture of calcium carbonate ($CaCO_3$ (analytical grade), Sigma Aldrich) and dicalcium phosphate anhydrous (monetite, DCPA) ($CaHPO_4$ (Ph.Eur., Fluka) at 1450°C for 5 hours. After cooling, the product was crushed by milling in a planetary ball mill (Fritsch) for 2 hours and phase purity was determined using the X-ray powder diffraction (XRD) analysis. The particle size distribution of the TTCP was measured in methanol by laser scattering particle size analyzer (SYMPATEC HELOS). The modified TTCP with nanomonetite (TTCPMH) was prepared by the in situ reaction between TTCP and a diluted solution of the orthophosphoric acid (86%, analytical grade, Merck) in ethanol + water (sample A, 9:1) mixture. Reaction was carried out in the planetary ball mill with agate balls and vessel for 30 min. The orthophosphoric acid solution/TTCP ratio was 1. The H_3PO_4 was added at such an amount that the final Ca/P mole ratio in powder mixture equals 1.67, which corresponds to the Ca/P mole ratio in hydroxyapatite. The effect of sodium dodecyl sulfate (SDS, Merck, for synthesis) was evaluated on TTCPMH-B samples – 5 g of powder sample was immersed into SDS methanol solution (0.6 mg/mL) and slowly mixed for 20 hours. The SDS concentration was under the solubility limit of SDS in methanol [12]. Powder was filtered and dried at 105°C for 1 hour. The amount of adsorbed SDS was determined as the difference between its content in the starting solution and filtrate using the methylene blue method [13]. The average amount of SDS adsorbed in the powder sample was 0.51±0.03 mg SDS/g powder cement. The control cement powder mixture was prepared by the mechanical mixing of TTCP and DCPA at a mole ratio of 1:1 in ethanol.

The compressive strength (CS) was measured for 10 samples of each type on a universal testing machine (LR5K Plus, Lloyd Instruments ltd.) at a crosshead speed of 1 mm/min and 10 mm/min respectively. The 4% NaH_2PO_4 (analytical grade, Sigma-Aldrich) solutions were used as hardening liquids. The powder to liquid ratio was 2. The powder mixture and resulting pastes were packed in stainless cylindrical form (6 mm D × 12 mm H). Samples were hardened in 100% humidity at 37°C for 10 min, soaked in 0.9% NaCl (analytical grade, Sigma-Aldrich) solution at 37°C for 1 week and dried at 100°C for 2 hours.

The pH values in the CPC slurries prepared by mixing 200 mg CPC powder in 50 mL of 0.9% NaCl solution were continuously measured using a pH-meter (WTW, Inolab 720) with Sentix 41 combined electrode

The phase compositions of samples during hardening in 0.9% NaCl solution were analyzed by X-ray diffraction analysis (Philips X´ PertPro, using Cu Kα radiation) and FTIR spectroscopy (Shimadzu, IRAffinity1, 400 mg KBr + 1 mg sample). The morphology and particle size of powder samples were observed by transmission electron microscopy (JEOL JEM 2100 F). The microstructures of fractured surfaces of samples after 7 days of

hardening and surfaces after 1 day of culture in α-MEM were observed by field emission scanning electron microscopy (JEOL FE SEM JSM-7000F). Densities of samples were calculated from their weights and dimensions. The setting times (ST) of the cement pastes were evaluated using the tip (1 mm diameter) of a Vicat needle with a 400 g load (according to ISO standard 1566), and fails to make a perceptible circular indentation on the surface of the cement.

Pre-osteoblastic MC3T3-E1 cells were (ECAAC, Sallisbury, UK) grown in α-modification Minimum essential medium (αMEM) with 10% fetal bovine serum (FBS, Sigma-Aldrich) at 95% humidity, 5 vol.% CO_2 and 37°C in an incubator (Memmert). After cells reached about 80% confluence, they were harvested by trypsinization with 0.25 % Trypsin-EDTA (Sigma-Aldrich) solution. TTCPMH pastes prepared by mixing with hardening liquid were hardened for 1 hour at 37°C and seeded with $2.0x10^4$ cells in 500 µl of complete medium with osteogenic supplements L - ascorbic acid (Sigma-Aldrich, 50 µg/ml), 50 nM Dexamethasone, 10 mM β-glycerophosphate and ATB-Antimycotic (Penicillin, Streptomycin, Amphotericin) solution (Sigma-Aldrich), cultured at 37°C in 5 vol.% CO_2 and 95% humidity in an incubator. The cell proliferation was examined using tetrazolium salt solution (MTS test, Cell titer 96 aqueous one solution cell proliferation assay, Promega, Madison, USA) and samples were evaluated for 48 hours, 5 and 10 days of culture in 48-well tissue culture plate (Santa Cruz Biotechnology, Santa Cruz, USA). The intensity of colouring, which characterizes the formazan concentration in the culture medium, was evaluated using a UVVIS spectrophotometer (Shimadzu 1800) at a wavelength of 490 nm. The pure complete culture medium was used as a blank. The acridine orange (AO), (Sigma-Aldrich) was used to stain the MC3T3 cells proliferated on samples prepared from hardened pastes. After 5 days of cultivation, the samples were stained with 0.01% AO solution for 2 minutes in the dark. The cells on substrates were observed using a fluorescence microscope (Leica DM IL LED, blue filter) for investigation of the cell distribution on samples. The relative initial cell attachment on hardened samples was calculated as the ratio of cell number in suspensions after 4 hours of cultivation in α-MEM to the starting cell number in suspensions (or seeding density) of $4x10^5$ cells per well. The cell number was calculated by a Neubauer hemacytometer. The ALP activity of osteoblasts was determined using the phosphatase substrate (Sigma-Aldrich, 5 mg tablet in 5mL diethanolamine buffer, pH=9.8) in cell lysates after lysis with a buffer (0.1 % Triton X-100, 1 mM $MgCl_2$ a 20 mM Tris). The 100 µL phosphatase substrate solution was added to 100 µL of cell lysate and the mixture was incubated at 37°C for 1h. The alkaline phosphatase reaction was be stopped by the addition of 50 µl of 3 M NaOH. ALP activity was measured by the amount of released p-nitrophenol after catalysis of the p-nitrophenol phosphate. The concentration of p-nitrophenol was determined from the calibration curve using UVVIS spectrophotometry at 405 nm. The ALP activity was expressed in nanomoles of p-nitrophenol/min/µg of protein. The content of proteins in samples was determined by Bradford's method with Coomasie blue G250 as the complexing agent [14, 15]. The statistical evaluation of results (n=3) was done using ANOVA analysis at level $\alpha = 0.05$.

RESULTS AND DISCUSSIONS

The morphology of TTCPMH particles is shown in Fig.1. The origin TTCP particles are irregularly shaped with the average particle size around 7 µm (Fig.1a). Particles have smooth surfaces, which is the result of crushing and grinding of sintered particle agglomerates obtained by a high temperature solid state synthesis of tetracalcium phosphate.

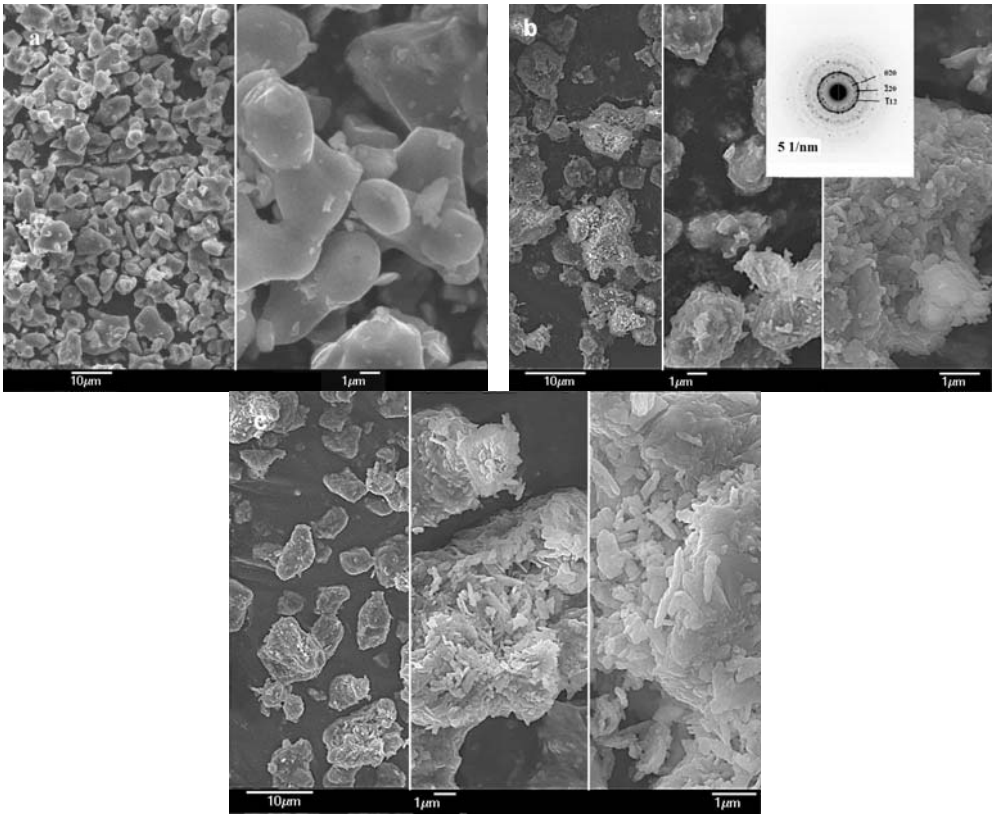

Fig.1. Morphology of TTCPMH particles observed by electron microscopy (a: origin TTCP particles; b: TTCPMH-A with the selected area electron diffraction; c:TTCPMH-B).

On the surfaces of origin TTCP phase are clearly visible aggregates of globular fine particles of new phase. A more compact surface layer of the secondary phase with particles up to 200 nm in size was observed in TTCPMH-A powder (Fig.1b). A highly porous surface texture with long needle-like particles is visible in TTCPMH-B powder (Fig.1c), which shows the exfoliation of particles from agglomerates. In the electron diffractogram (in inset), the polycrystalline character of nanoparticles and the formation of monetite phase were confirmed. Note that the nanomonetite particles were homogeneously distributed in powder cement mixture or they were tightly bonded to the surface of origin TTCP particles.

In TTCPMH-A sample (Fig.2a), the compact microporous microstructure, which corresponds with the morphology of origin powder particles, was found with hardly distinguished thin needle-like particles of hydroxyapatite phase after 7 days of hardening in 0.9% NaCl at 37°C. The comparison between cement samples shows that the SDS adsorption at surfaces of the powder cement precursor (Fig.2b) causes an increase of porosity with a rise in fraction of larger, approximately 10 μm pores. Besides this, thicker particles of plate-like morphology joined into the form of spherical hollow agglomerates can be found in the microstructure. Neira et al. [16] prepared CPC by mixing intensively milled dicalcium phosphate dihydrate (DCPD) and TTCP powder phases and globular nanohydroxyapatite particles observed in cement microstructures after soaking in distilled water.

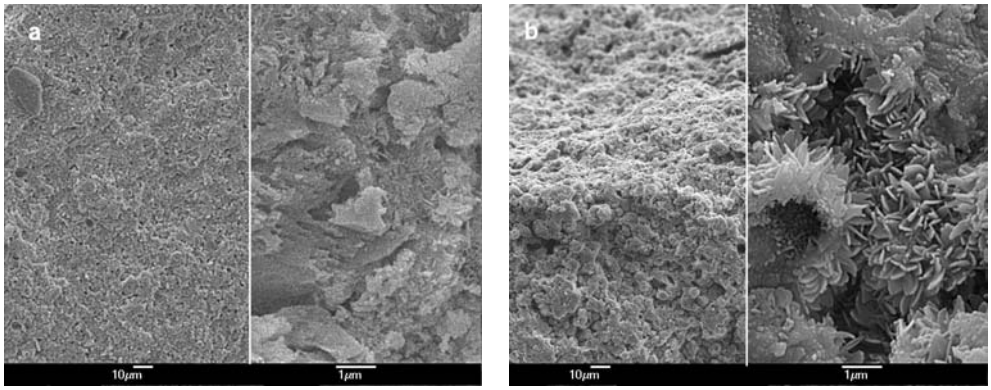

Fig.2. Microstructure of cements after 7 days of hardening in 0.9% NaCl at 37°C (a: TTCPMH-A; b: TTCPMH-B).

The specific surface areas of TTCPMH-samples rose approximately fourfold in comparison with pure TTCP specific area about 2.37 m^2/g. The specific area of particles in the TTCPMH-A sample (3.80±0.11 m^2/g) was lower than in the sample with an addition of SDS (6.91±0.28 m^2/g). This result corresponds with SEM observations, where TTCPMH-A sample had more compact agglomerates and some degree of agglomerate disaggregation with the rise in porosity were found after SDS addition.

The XRD analysis of TTCPMH cement powders verified formation of the monetite phase, which demonstrate lines from reflections of (020), (220) and (112) monetite planes (JCPDS 09-0080) at 2Θ equal 26.5 and 30.2° between lines from reflections of the starting TTCP phase (JCPDS 25-1137) (Fig.3, curve 1). The nanosize character of monetite phase clearly shows the overlap lines from (020) and (220) reflections. No differences in rates of cement mixtures` transformation to nanohydroxyapatite were observed between TTCPMH powders with and without adsorbed SDS. Note that the final phase in hardened cements was he nanocrystalline hydroxyapatite (JCPDS 24-0033) (Fig.3, curve 4). Traces of TTCP was found in the final cement after 7 days of TTCP-MCPM mixture hardening [17].

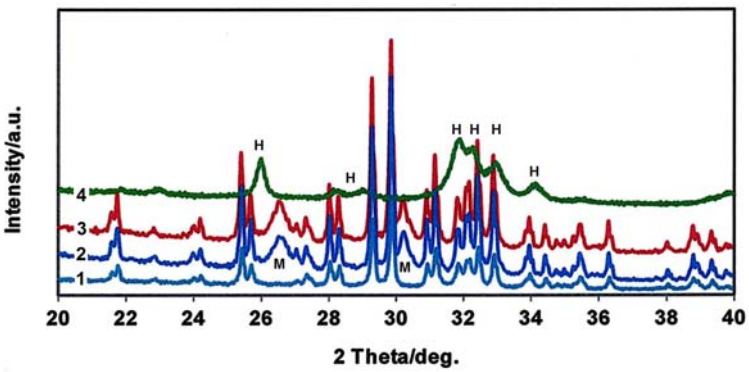

Fig.3. XRD patterns of TTCPMH powder mixtures after 30 mins of reaction milling (a) (1: origin TTCP phase; 2: TTCPMH-A; 3: TTCPMH-B) and after 24 hours of hardening in 0.9% NaCl at 37 °C (4) (M:monetite, H:hydroxyapatite).

FTIR spectra of the TTCPMH samples and pure TTCP phase are shown in Fig.4. From the comparison of spectra it results that the ν_3 stretching vibrations of PO_4^{3-} group (between 987 and 1100 cm^{-1}; ν_1 symmetric stretching vibrations around 950 cm^{-1}) similarly as ν_4 and ν_2 deformation O-P-O vibrations under 700 cm^{-1} of origin TTCP [18] were not changed after reaction milling. Besides this, the peaks from P-OH plane bending vibrations at around 1410 and 1350 cm^{-1}, and shoulders at 1130 and 890 cm^{-1} characteristic for ν_3 stretching vibrations of P-O and P-O(H) monetite bonds were found in the spectra of TTCPMH samples [19]. In the FTIR spectra of TTCPMH-A cement sample after hardening (Fig.4, curve 2), the characteristic vibrations of the PO_4^{3-} group in hydroxyapatite from antisymmetric (ν_3) and symmetric (ν_1) P-O stretching vibrations located at 1034, 1090 and 962 cm^{-1}, O-P-O bending (ν_4) vibrations at 564 and 603 cm^{-1}, and the librational mode of OH group at 632 cm^{-1} were observed. The presence of low intensive peaks at 1432, 1482 and 870 cm^{-1}, which characterize ν_2 and ν_3 vibrations of CO_3^{2-} group in hydroxyapatite, verify the formation of carbonated B-type hydroxyapatite with CO_3^{2-} substitution for PO_4^{3-} groups [20, 21].

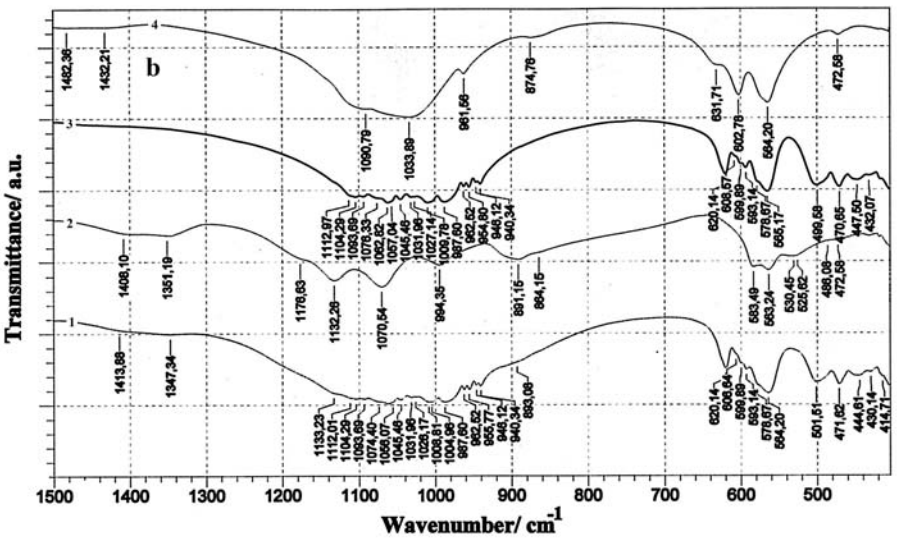

Fig.4. FTIR spectra of TTCPMH powder mixtures after 30 minutes of reaction milling (a) (3: origin TTCP phase; 2: monetite;1:TTCPMH-A; 4: after 24 hours of hardening in 0.9% NaCl at 37°C.

A higher CS (35.4 MPa) was measured in TTCPMH-A cement with a more dense microstructure without distinguished hydroxyapatite particles and with a low separation of individual particle agglomerates. In the case of the sample with SDS addition, the CS was almost the same as in the TTCP control cement (18 MPa). As resulting from the SEM analysis, a strong separation of particle agglomerates was observed in this sample and the rise in microporosity caused by the formation of hollow particles with possible air trapped during cement paste preparation because of the change in surface tension. The presence of SDS on particle surfaces was the reason for approx. 30% rise of setting time (to 11 minutes) in comparison with the pure TTCPMH-A cement. The reason of this effect can be the formation of intermediates between Ca^{2+} ions and DS^- ions, which can decelerate the hardening process and summary reaction rate in the system. A high CS (up to 60 MPa) was

achieved in CPC fabricated from TTCP-DCPA powder mixture with an orthophosphoric acid solution as the hardening liquid but more acidic pH values were measured at the beginning of setting [2, 22]. It has been found that CS´s TTCP-DCPD cements were very low and the setting time was not affected by the presence of SDS in the cement paste [10].

A small lowering of both maximum pH values to 7.8 and 8.2 as well as ones after 24 hours to 7.5 and 7.8 were observed in TTCPMH-A and B cement pastes. Baviere et al. [23] showed the influence of SDS concentration on the formation of calcium dodecyl sulfate and tolerance of SDS to the increase of free Ca^{2+} ions in solution at higher SDS concentrations because of the association between micelles and Ca^{2+} ions. Besides this, there has been shown a rise of this tolerance with an amount of NaCl in the solution and strong reduction of the critical micellar concentration (CMC). The phosphate ions were released from the hydroxyapatite surface during the SDS adsorption and both the phosphate ion concentration and pH rose with SDS amount in solution [24]. Shimabayashi et al. [25] verified the competitive adsorption between DS^- and phosphate ions on the hydroxyapatite surface as well as a strong reduction of the release of phosphate or calcium ions with NaCl or HPO_4 concentrations in solution. Thus the

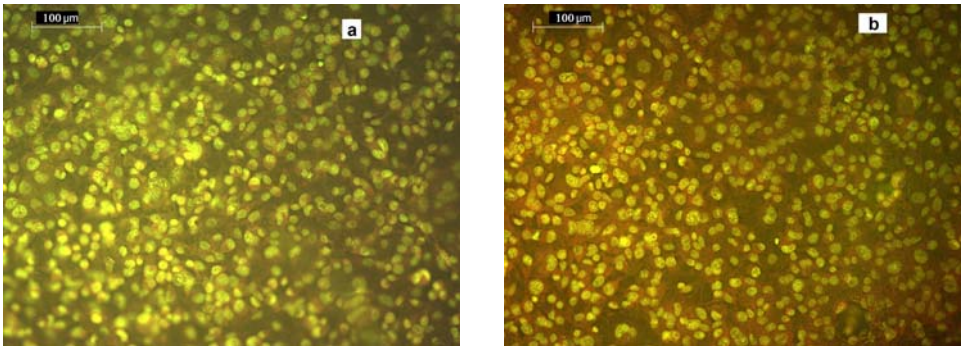

Fig.5. Distribution of osteblasts on cement surfaces after 4 hours of proliferation at 37°C in 5% CO_2 and 90% humidity (optical fluorescence micrographs (acridine orange staining) (a: TTCPMH-A; b: TTCPMH-B).

SDS interacts with Ca^{2+} ions, which are released during the TTCP hydrolysis in water solutions and the concentration of OH^- ions rise in solution, which causes the shift of solution pH to a more basic region. The initial cell attachment on cement scaffolds after 4 hours of incubation at 37°C and 5 vol.% CO_2 atmosphere was characterized as the relative number of osteoblast adhered on the surface of hardened cement samples. A small decrease was found in the number of adhered osteoblasts in sample B (treated with SDS), and the relative adherences of cells were around 65% of seeding density ($4x10^5$ cells per well). The high density of osteoblasts after 4 hours of culture on sample surfaces can be visible in Fig.5. No initial cytotoxicity, which could affect the cell morphology or cell spreading, was observed. Osteoblasts were well spread on surfaces with clearly visible filopodia.

MTS tests of osteoblast viabilities on cement pastes after 1 hour setting at 37°C are shown in Fig.6 a. From comparison it results that proliferation was very similar on both cement scaffolds after 48 hours of incubation. An approximate double growth of the osteoblast population was observed after 5 days of culture in TTCPMH-A but a decrease was found in sample B. After 10 days, a small reduction in cell viability was measured in the samples. The surfaces of substrates after 48 hours of cell proliferation are shown in

Fig.7. A denser matrix was formed by cells on surface cement substrates. Note that the thickness of the produced extracellular matrix was around 1-4 μm and almost fully covers the surface of hydroxyapatite particles. The fast drop of osteoblast ALP activities on hardened cement pastes was observed with prolongation of incubation (Fig.6 b). The ALP activities were sometimes higher in cements TTCPMH-A after 24 hours of cultivation than after 5 days and a much lower ALP activity of cells was found in sample B. The ALP activity of osteoblasts on DCPD-TTCP depends on the degree of their differentiation and the highest activity is measured during first stages of differentiation, in which collagen type I is synthesized [26].

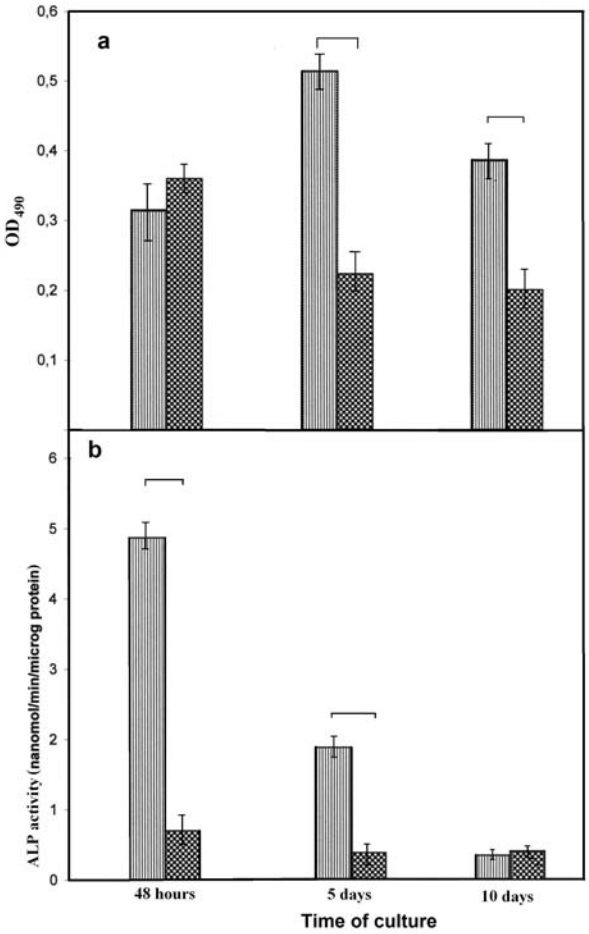

Fig.6. Osteoblast proliferation on cement substrates measured by formazan production in MTS test (a) and the ALP activity (b) of osteoblasts during proliferation on cement substrates (TTCPMH-A, TTCPMH-B, mean±SD, n = 3, statistical significant differences, $p>0.05$).

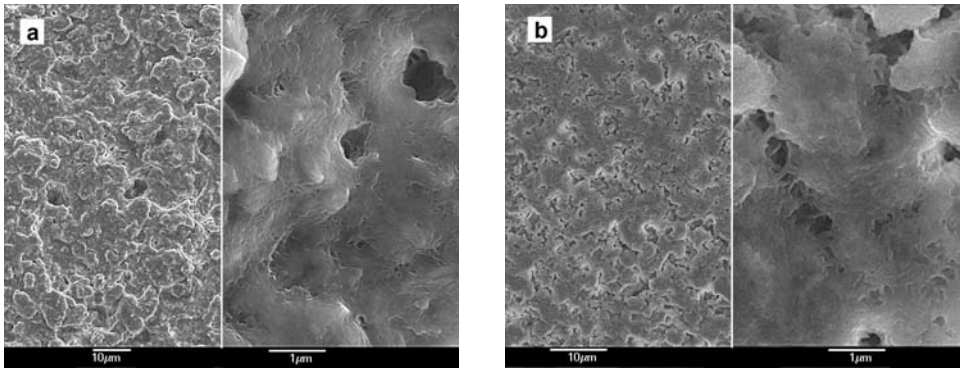

Fig.7. Surface texture of cement samples after 48 hours of cell proliferation (a: TTCPMH-A, b: TTCPMH-B).

In Figure 8, optical micrographs of osteoblasts proliferated on scaffolds after 5 days of cultivation are shown. It is clearly visible that the largest number of cells interconnected in the form of bundles was on the surface of TTCPMH-A scaffolds.

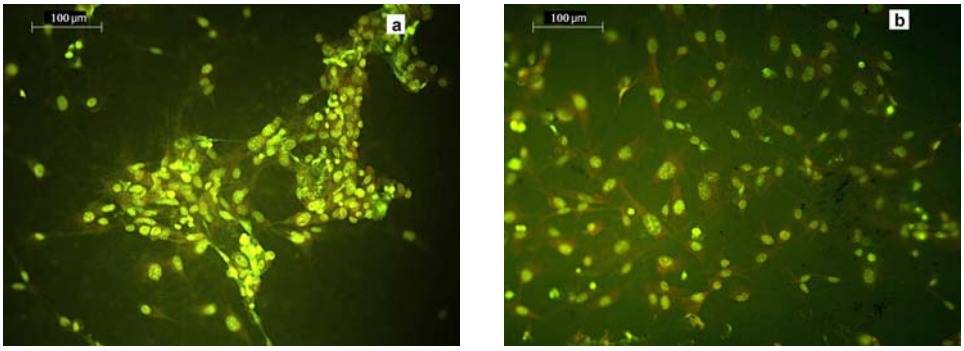

Fig.8. Distribution of osteblasts on cement surfaces after 5 days of proliferation at 37°C in 5% CO_2 and 90% humidity (optical fluorescence micrographs (acridine orange staining) (a: TTCPMH-A; b:TTCPMH-B).

On the other hand, osteoblasts were very well spread with a long mutually joined filopodia and uniformly distributed on the surface of TTCPMH-B scaffolds. The cell viability on CPC was more significantly influenced by the surface morphology of cements than their physico-chemical properties [17]. Ehara et al. showed that TTCP does not affect the proliferation rate of osteoblasts and promote both the increase in extracellular matrix formation and a shift to a more differentiated state [9]. There has been reported a good interaction between the filopodia of well-flattened spread cells and the nanocrystallized hydroxyapatite regions [27]. The cell proliferation, total protein content and ALP activity were significantly reduced by the irregular and rough surface of hydroxyapatite [28]. We believe from the above facts that the used pre-osteoblasts were more differentiated after seeding, which caused the reduction in ALP cement activities with prolonged cultivation. Besides this, the surface roughness of TTCPMH-B substrates and the size of the plate-like hydroxyapatite particles were higher than in TTCPMH-A.

CONCLUSION

CPC cement powders composed of TTCP and nanomonetite phases characterize the reduction in pH values during cement paste hardening in comparison with the conventional cement powder mixture. The SDS adsorption on surfaces of powder particles in cement mixtures caused a rise in setting time, a decrease of mechanical properties, a rise in cement porosity and it influenced the particle morphology in cement. No differences in XRD patterns or FTIR spectra were found between cement powder mixtures and traces hydroxyapatite were verified only. Excellent initial cell attachment without visible cytotoxicity and good osteoblast proliferation were observed on the surface of cements. The cement with SDS addition had lower osteoblast proliferation and ALP activity with prolongation of culturing.

Acknowledgements

This work was supported by the Slovak Grant Agency of the Ministry of Education of the Slovak Republic and the Slovak Academy of Sciences, Project No. 2/0026/11 and within the framework of the project „Advanced implants seeded with stem cells for hard tissues regeneration and reconstruction“, which is supported by the Operational Program “Research and Development” financed through European Regional Development Fund.

REFERENCES

[1] Brown, WE., Chow, LC.: US Patent No. 4518430 (1985)
[2] Chen, WC., Ju, CP.,Chern Lin, JH.: J. Oral. Rehabil., vol. 34, 2007, p. 541-551
[3] Gbureck, U., Knappe, O., Hofmann, N., Barralet, JE.: J. Biomed. Mater. Res. Part B: Appl. Biomater., vol. 83B, 2007, p. 132–137
[4] Dagang, G., Kewei, X., Haoliang, S., Yong, H.: J. Biomed. Mater. Res., vol. A 77, 2006, p. 313-323
[5] Medvecký, Ľ., Štulajterová, R., Briančin, J., Ďurišin, J.: Mater. Sci. Eng., vol. C 29, 2009, p. 2493-2501
[6] Tenhuisen, KS., Brown, PW.: J. Biomed. Mater. Res., vol. 36, 1997, p. 233-241
[7] Guo, H., Su, J., Wei, J., Kong, H., Liu, C.: Acta Biomater., vol. 5, 2009, p. 268–278
[8] Wang, JC., Ko, CL., Hung, CC., Tyan, YC., Lai, CH., Chen, WC., Wang, CK.: J. Dent., vol. 38, 2010, p. 158-165
[9] Ehara, A., Ogata, K., Imazato, S., Ebisu, S., Nakano, T., Umakoshi, Y.: Biomaterials, vol. 24, 2003, p. 831–836
[10] Hesaraki, S., Nemati, R.: J. Biomed. Mater. Res. Part B: Appl. Biomater., vol. 89B, 2009, p. 342–352
[11] Sarda, S., Nilsson, M., Balcells, M., Fernandez, E.: J. Biomed. Mater. Res., vol. 65A, 2003, p. 215–221
[12] Miyata, I., Takada, A., Yonese, M., Kishimoto, H.: Bull. Chem. Soc. Jpn., vol. 63, 1990, p. 3502-3507
[13] Hayashi, K.: Anal. Biochem., vol. 67, 1975, p. 503-506
[14] Bradford, MM.: Anal. Chem., vol. 72, 1976, p. 248-254
[15] Zor, T., Selinger, Z.: Anal. Biochem., vol. 236, 1996, p. 302-308
[16] Neira, IS., Kolen'ko, YV., Lebedev, OI., Van Tendeloo, G., Gupta, HS., Matsushita, N.,. Yoshimura, M., Guitián, F.: Mat. Sci. Eng., vol. C 29, 2009, p. 2124–2132
[17] Van den Vreken, NM., Pieters, IY, Declercq, HA., Cornelissen, MJ., Verbeeck, RM.: Acta Biomater., vol. 6, 2010, 617–625
[18] Moseke, C., Gbureck, U.: Acta Biomater., vol. 6, 2010, p. 3815–3823

[19] Xu, J., Butler, IS., Gilson, DFR.: Spectrochim. Acta Part A, vol. 55, 1999, p. 2801–2809
[20] Krajewski, A., Mazzocchi, M., Buldini, PL., Ravaglioli, A., Tinti, A., Taddei, P., Fagnano, C.: J. Molecular. Struc., vol. 744-747, 2005, p. 221-228
[21] Apfelbaum, F., Diab, H., Mayer, I., Featherstone, JDB.: J. Inorg. Biochem., vol. 45, 1992, p. 277-282
[22] Wang, JC, Ko, CL., Hung, CC., Tyan, YC., Lai, CH., Chen, WC., Wang, CK.: J. Dent., vol. 38, 2010, p. 158-165
[23] Baviere, M., Bazin, B., Aude, R.: J. Coll. Inter. Sci., vol. 92, 1983, p. 580-583
[24] Shimabayashi, S., Tanaka, H., Nakagaki, M.: Chem. Pharm. Bull., vol. 34, 1986, no. 11, p. 4474-4478
[25] Shimabayashi, S., Tanaka, H., Nakagaki, M.: Chem. Pharm. Bull., vol. 35, 1987, no. 6, p. 2171-2176
[26] von Wilmowsky, C., Moest, T., Nkenke, E., Stelzle, F., Schlegel, KA.: Oral Maxillofac. Surg. DOI 10.1007/s10006-013-0398-1
[27] Lu, YP., Chen, YM., Li, ST., Wang, JH.: Acta Biomater., vol. 4, 2008, p. 1865–1872
[28] Rosa, AL., Beloti, MM., van Noort, R.: Dent. Mater., vol. 19, 2003, p. 768–772